

# Dietary Supplementation with the Probiotic SF68 Reinforces Intestinal Epithelial Barrier in Obese Mice by Improving Butyrate Bioavailability

Laura Benvenuti, Vanessa D'Antongiovanni, Carolina Pellegrini, Matteo Fornai,\*  
Nunzia Bernardini, Chiara Ippolito, Cristina Segnani, Clelia Di Salvo, Rocchina Colucci,  
Alma Martelli, Lorenzo Flori, Vincenzo Calderone, Gianfranca Carta, Emilia Ghelardi,  
Marco Calvigioni, Adelaide Panattoni, Raffaella Coppolecchia, Achille Arini,  
and Luca Antonioli

**Scope:** Modifications in intestinal microbiota and its metabolites, the short-chain fatty acids (SCFA) are main factors altering intestinal epithelial barrier integrity and eliciting the onset of a meta-inflammation observed in obesity. The present study is aimed at evaluating the efficacy of *Enterococcus faecium* (SF68) administration in counteracting the impairment of gut barrier and enteric inflammation in a model of diet-induced obesity, characterizing the molecular mechanisms underlying such beneficial effects.

**Methods and Results:** Male C57BL/6J mice, fed with standard diet (SD) or high-fat diet (HFD), are treated with SF68 ( $10^8$  CFU day<sup>-1</sup>). After 8 weeks, plasma interleukin (IL)-1 $\beta$  and lipopolysaccharide binding protein (LBP) are measured, analysis of fecal microbiota composition and butyrate content as well as intestinal malondialdehyde, myeloperoxidase, mucins, tight junction protein, and butyrate transporter expression are investigated. After 8 weeks, SF68 administration counteracts the body weight gain in HFD mice, reducing plasma IL-1 $\beta$  and LBP. In parallel, SF68 treatment acts against the intestinal inflammation in HFD-fed animals and improves the intestinal barrier integrity and functionality in obese mice via the increase in tight junction protein and intestinal butyrate transporter (sodium-coupled monocarboxylate transporter 1) expression.

**Conclusions:** Supplementation with SF68 reduces intestinal inflammation and reinforces the enteric epithelial barrier in obese mice, improving the transport and utilization of butyrate.

## 1. Introduction

Obesity is a multifactorial pathological condition characterized by an excess body fat often associated with a large number of debilitating and life-threatening disorders, affecting, along with overweight, over a third of the world's population.<sup>[1]</sup> A number of evidence reported that beyond an abnormal fat accumulation, the excessive intake of foods with high energy density can lead to a low-intensity chronic systemic inflammation (meta-inflammation), a common root to several obese-related comorbidities, including type 2 diabetes, cardiovascular disease, non-alcoholic fatty liver disease, and cancer.<sup>[2]</sup>

Over the years, increasing efforts have been addressed to better understand and characterize the molecular pathway underlying the onset and development of obesity, aimed at identifying novel route for therapeutic intervention.<sup>[3]</sup> Interestingly, a number of clinical and preclinical evidence identified a failure in the relationship of mutual benefit occurring between the host and the gut microbiota,

L. Benvenuti, V. D'Antongiovanni, C. Pellegrini, M. Fornai, N. Bernardini, C. Ippolito, C. Segnani, C. Di Salvo, L. Antonioli  
Department of Clinical and Experimental Medicine  
University of Pisa  
Pisa Italy  
E-mail: matteo.fornai@unipi.it

N. Bernardini  
Interdepartmental Research Center "Nutraceuticals and Food for Health"  
University of Pisa  
Pisa Italy

R. Colucci  
Department of Pharmaceutical and Pharmacological Sciences  
University of Padova  
Padova Italy

A. Martelli, L. Flori, V. Calderone  
Department of Pharmacy  
University of Pisa  
Pisa Italy

The ORCID identification number(s) for the author(s) of this article can be found under <https://doi.org/10.1002/mnfr.202200442>

© 2023 The Authors. Molecular Nutrition & Food Research published by Wiley-VCH GmbH. This is an open access article under the terms of the Creative Commons Attribution-NonCommercial-NoDerivs License, which permits use and distribution in any medium, provided the original work is properly cited, the use is non-commercial and no modifications or adaptations are made.

DOI: 10.1002/mnfr.202200442

as a hallmark typically associated with obesity.<sup>[4]</sup> In this regard, alterations in intestinal microbiota and its metabolites, the short-chain fatty acids (SCFA), have been identified among the main factors influencing early inflammatory events associated with obesity and metabolic dysfunction.<sup>[5]</sup> In particular, set of metagenomic and biochemical analyses allowed to highlight the presence of an imbalanced gut microbiota in murine model of diet-induced obesity as well as in obese patients,<sup>[6]</sup> in association with an altered proportion in luminal and fecal SCFA production.<sup>[7]</sup> Such luminal alterations represent prodromal events eliciting fluctuations in the intestinal epithelial barrier integrity, thereby facilitating the translocation of immunogenic products (i.e., lipopolysaccharide, peptidoglycan, whole bacteria, and other toxins) in the enteric *lamina propria* and the bloodstream, triggering the onset and maintenance of a meta-inflammation typically observed in obese subjects.<sup>[8]</sup>

Recent studies strongly indicated that the manipulation of the composition of the microbial ecosystem in the gut via prebiotics and/or probiotics might be a viable way in the treatment of obesity.<sup>[9]</sup> Set of preclinical studies performed in murine models of diet-induced obesity reported the beneficial effects of a probiotic supplementation in regulating body weight and in counteracting proinflammatory gene expression in the adipose tissue.<sup>[10,11]</sup> In parallel, although not completely understood, it has been observed that the administration of probiotics (i.e., *Lactobacilli* and *Escherichia coli* Nissle 1917) ameliorated the functionality of the intestinal barrier, modulating the expression of numerous genes encoding adherence junction proteins, leading to the restoration of the tight junction complex.<sup>[12]</sup> Moreover, *Enterococcus faecium* SF68 (SF68) has been demonstrated to reduce symptoms of intestinal inflammation in both pre-clinical and clinical studies.<sup>[13–16]</sup> In particular, it has been reported an ameliorative effect in case of antibiotic-associated diarrhea.<sup>[15,16]</sup>

Despite these encouraging results, several gaps remain about our understanding of how probiotics modulate gut microflora to protect against the mucosal and the immune/inflammatory enteric disorders associated with obesity.

Based on these premises, the present study has been designed to evaluate the efficacy of SF68 administration in counteracting and preventing the impairment of gut barrier and the onset of enteric inflammation in a mouse model of diet-induced obesity, characterizing the molecular mechanisms underlying such beneficial effects.

G. Carta  
Department of Biomedical Sciences  
University of Cagliari  
Cagliari Italy

E. Ghelardi, M. Calvigioni, A. Panattoni  
Department of Translational Research and New Technologies in  
Medicine and Surgery  
University of Pisa  
Pisa Italy

R. Coppolecchia, A. Arini  
Cerbios Pharma-SA  
Lugano Switzerland

## 2. Experimental Section

### 2.1. Animals and Diet

C57BL/6 male mice (20–22 g body weight), 5-week-old, were provided by ENVIGO S.r.l (San Pietro al Natisone UD, Italy) and used during the study. They were housed six in a cage in a temperature-controlled room on a 12-h light cycle at 22–24 °C, and 50%–60% humidity and not used for at least 1 week. They were handled and cared following the European Community Council Directive 2010/63/UE, transposed by the Italian Government. The study was approved by the Italian Ministry of Health (Authorisation N° 955/2018-PR).

### 2.2. Experimental Design

To induce obesity, standard diet (SD, 18% calories from fat; TD.2018), administered during the adaptation period to all mice, was replaced with a high-fat diet (HFD, 60% calories from fat, TD.06414) for 8 weeks. HFD provides 21.4% kcal as carbohydrate, 18.3% kcal as protein, and 60.8% kcal as fat (5.1 kcal g<sup>-1</sup>), instead SD provides 58% kcal as carbohydrate, 24% kcal as protein, and 18% kcal as fat (3.1 kcal g<sup>-1</sup>). Body weight was measured once a week from the first day of the study. At the end, animals were anaesthetized and sacrificed. Blood samples and tissue samples were collected and stored at –80 °C for further analysis. Animals were randomly divided into six groups, each composed by ten mice, as follow: SD or HFD plus vehicle for 8 weeks, SD or HFD with the probiotic starting from the fourth week (treatment 4 + 4), SD or HFD plus probiotic for 8 weeks. SF68 was administered via oral gavage, at the dose of 10<sup>8</sup> CFU day<sup>-1</sup>, as previously reported.<sup>[17]</sup> The experimental design could be represented schematically in the Supplemental Figure S1.

### 2.3. Plasma Interleukin-1 $\beta$ and lipopolysaccharide binding protein (LBP) Levels

Interleukin (IL)-1 $\beta$  and lipopolysaccharide binding protein (LBP) levels in plasma were measured by ELISA (Prodotti Gianni, Milan, Italy), as previously described.<sup>[18]</sup> For the procedure, blood samples were centrifuged for 5 min at 4000 rpm at 2–8 °C and, after the centrifugation, supernatant were collected. Aliquots (100  $\mu$ L) were used for the assay. IL-1 $\beta$  levels were expressed as pg mL<sup>-1</sup> of plasma, while LBP levels were expressed as ng mL<sup>-1</sup> of plasma.

### 2.4. Analysis of Bacterial Populations in Fecal Samples

Firstly, genomic DNA extraction from fecal samples was performed using QIAamp PowerFecal Pro DNA Kit (QIAGEN, Hilden, Germany), following the manufacturer's protocol. The concentration of DNA was calculated at OD260 nm and DNA purity was estimated by determining the OD260/OD280 and OD260/OD230 ratio, by the spectrophotometer BioPhotometer D30 (Eppendorf). Then real-time quantitative PCR (RT-qPCR) was carried out. 16S rRNA gene-based qPCR analysis of extracted

DNAs was used to quantify the amount of total bacteria and of the main microbial phyla (i.e., *Firmicutes*, *Bacteroidetes*, *Actinobacteria*, and *Proteobacteria*) and genera (i.e., *Bacteroides*, *Fecalibacterium*, *Akkermansia*, *Lactobacillus*, and *Bifidobacterium*) represented in the fecal microbiota. qPCR reactions were led by using CFX96 Real-Time System (BioRad). Absolute quantification was executed using the CFX Manager Software (BioRad).

## 2.5. Evaluation of Fecal Butyrate

For butyrate analysis, feces were collected and kept at  $-80^{\circ}\text{C}$  until further processing. Up to 100 mg of frozen material was used and processed with 700  $\mu\text{L}$  of 1-butanol (ACROS Organics, Fisher Scientific) followed by 1 min of gentle vortexing and then kept for 50 min at RT. After centrifugation at  $300 \times g$  for 10 min, the supernatant was transferred to a glass tube containing 1 mL of Boron trifluoride-1-butanol solution ( $\approx 10\%$  in 1-butanol). Tubes were vortexed and kept at RT for 30 min. 2.5 mL of hexane, 1 mL of distilled water, and 0.2 mL of saturated sodium chloride solution were then added to the formulations and samples were vortexed and kept at RT for 50 min. An aliquot of the supernatant, hexane containing the butylated SCFA, was diluted 1:4 with methanol.

The identification and quantification were carried out by liquid chromatography-tandem mass spectrometry (LC-MS/MS). An Agilent 1100 HPLC system (Agilent, Palo Alto, CA, USA) was coupled to a mass spectrometry Agilent Technologies QQQ triple quadrupole 6420 equipped with an ESI source, using positive mode (ESI+). A C-18 Zorbax Eclipse Plus column (Agilent, Palo Alto, CA, USA) with 5  $\mu\text{m}$  particle size and  $50 \times 4.6$  mm was used with a mobile phase of  $\text{CH}_3\text{OH}/\text{H}_2\text{O}/\text{CHOOH}$  (70/30/0.1 v/v/v) at a flow rate of 0.5 mL  $\text{min}^{-1}$ .  $\text{N}_2$  was used as a nebulizing gas with a pressure of 50 psig, drying gas temperatures  $300^{\circ}\text{C}$  and flow of 11 L  $\text{min}^{-1}$ , and 4000 V capillary voltage. The precursor ion  $[\text{M} + \text{H}]^+$  was determined during a full scan in MS and then the obtained product ion (PI) was monitored for each transition in MRM mode in MS/MS. Parameters of source, such as collision energy (CE) and cone voltage or fragmentor (CV), have been optimized for each MRM transition. Butyl butyrate transitions was [145  $\rightarrow$  89].

The MassHunter workstation acquisition software was used to collect data, which was analyzed for quantitative and qualitative analysis. Sigma Chemicals Co. (St. Louis, MO, USA) provided butyric acid (Supelco) and butyl butyrate, boron trifluoride-1-butanol solution ( $\approx 10\%$  in 1-butanol), formic acid, *n*-hexane, water, methanol, and LiChrosolv gradient grade for liquid chromatography.

## 2.6. Histological Analysis

Formalin fixed and paraffin embedded full-thickness colonic samples were serially cross-sectioned (7  $\mu\text{m}$ ) and processed for hematoxylin & eosin for eosinophil detection, histochemical staining, and confocal immunofluorescence microscopy.

### 2.6.1. Histochemical Staining

The sections were stained with Alcian Blue (1% in 3% acetic acid) followed by the periodic acid-Schiff (PAS) reaction and then

counterstained with hematoxylin, to detect the acidic and neutral mucin which resulted blue- and magenta-stained, respectively, as previously reported.<sup>[19]</sup>

### 2.6.2. Confocal Immunofluorescence

Immunofluorescence staining was performed to detect colonic claudin-1-positive tight junctions, as previously reported<sup>[21]</sup>. Briefly, sections were sequentially incubated with Protein Block Serum Free (DakoCytomation, Glostrup, Denmark), rabbit polyclonal anti-claudin-1 [1:600] (code: ab15098; Abcam, Cambridge, UK) overnight at  $4^{\circ}\text{C}$ , treated with biotinylated secondary antibody ([1:300]; code: BA-1000; VectorLab; Burlingame, CA, USA) and Alexa Fluor 555 conjugated streptavidin ([1:300]; code: S32355; Invitrogen, Eugene, OR, USA) and finally nuclear counterstaining with TO-PRO3 (code: T3605, Invitrogen).

### 2.6.3. Image Analysis

Histological data were quantitatively estimated by two blind histologists (C.S. and C.I.). The density of eosinophils was evaluated in the *tunica mucosa/submucosa* by a Leica DMRB light microscope (object 40 $\times$ ), equipped with a DFC480 digital camera (Leica Microsystems, Mannheim, Germany), and expressed as cell number per square millimeter, as described previously<sup>[20]</sup>. Alcian blue/PAS and claudin-1 immunofluorescent stainings in the *tunica mucosa* were acquired by a Navigator mode of Leica TCS SP8 microscope (objects: 20 $\times$ ), equipped with a Leica DFC 7000 T camera for brightfield images (Leica Microsystems), and a Leica TCS SP8 confocal laser-scanning microscope (objects: 63 $\times$  oil lens; Leica Microsystems), respectively. Positive areas were estimated by the Image Analysis System "Leica Application Suite (L.A.S.) X software, as percentage of  $\Sigma$  of positive-stained area/ $\Sigma$  of tissue area examined (percentage of positive pixels) and quantified as the ratio of the final value over the initial value (fold change). Data were expressed as mean  $\pm$  SEM.

## 2.7. Tissue Myeloperoxidase (MPO) Levels

MPO levels in colonic tissues were measured by ELISA (Prodotti Gianni, Milan, Italy), as previously described.<sup>[20]</sup> Colonic specimens, previously stored at  $-80^{\circ}\text{C}$ , were homogenized on ice with a polytron homogenizer (QIAGEN, Milan, Italy). The homogenates were centrifuged at  $4^{\circ}\text{C}$  for 15 min at 12 000 rpm. Aliquots (100  $\mu\text{L}$ ) of the supernatants were then utilized for the assays. MPO levels were expressed as ng  $\text{mg}^{-1}$  of tissue.

## 2.8. Tissue Malondialdehyde (MDA) Levels

The MDA concentration in intestinal specimens was measured in order to achieve a quantitative estimate of mucosal infiltration by polymorphonuclear cells. The assay was carried out as mentioned previously.<sup>[18]</sup> Intestinal tissues were weighted, minced,

and homogenized with a polytron homogenizer in 2 mL of cold buffer (QIAGEN, Milan, Italy) and centrifuged at 1200 rpm for 10 min at 4 °C. The concentrations of MDA were measured using a colorimetric assay kit (Calbiochem, San Diego, CA, USA), with the findings expressed in nmol of MDA per mg of colonic tissue.

## 2.9. Western Blot Assays

Colonic tissues were weighed and then homogenized in lysis buffer (50 mg in 400 µL), using a polytron homogenizer (QIAGEN, Milan, Italy). Homogenates were spun by centrifugation at 12,000 rpm for 15 min at 4 °C, and the resulting supernatants were then separated from pellets and stored at –80 °C. Bradford assay was performed to quantify total proteins. Subsequently, proteins were separated onto a pre-cast 4%–20% polyacrylamide gel (Mini-PROTEAN TGX gel, BioRad) and transferred to PVDF membranes (Trans-Blot Turbo™ PVDF Transfer packs, BioRad). Membranes were blocked with 3% BSA diluted in Tris-buffered saline (TBS, 20 mM Tris-HCl, pH 7.5, 150 mM NaCl) with 0.1% Tween 20. Primary antibodies against β-actin (ab8227, Abcam), occludin (ab167161, Abcam), zonulin-1 (Ab96587, Abcam), claudin (ab15098, Abcam), toll-like receptor (TLR) 4 (ab22048, Abcam), TLR2 (ab213676, Abcam), nuclear factor-κB (NF-κB)-p65 (sc-8008, Santa Cruz), MyD88 (sc-136970, Santa Cruz), sodium-coupled monocarboxylate transporter 1 (SMCT1, BS-6106R, Bioss), monocarboxylate transporter 1 (MCT1, PA5-76687, Thermo Fisher), monocarboxylate transporter 4 (MCT4, PA5-106683, Thermo Fisher), and Histone deacetylase 1 (HDAC1, sc-81598, Santa Cruz) were used. Secondary antibodies were bought from Abcam (antimouse ab97040 and antirabbit ab6721). Protein bands were revealed with ECL reagents (Clarity Western ECL Blotting Substrate, BioRad), iBright Analysis software was used to perform the densitometry analysis.

## 2.10. Evaluation of Citrate Synthase Activity on Ileum

The frozen tissues, resulting from the different mice groups, were homogenized on ice in a cold buffer (sucrose 250 mM, Tris 5 mM, EGTA 1 mM, Triton X-100 0.02%; pH 7.4) with GentleMACS dissociator (Miltenyi Biotec, Bologna, Italy). Homogenates were centrifuged at 12,000 × g for 15 min at 4 °C (EuroClone, Speed Master 14 R centrifuge, Milan, Italy). The pellets were discarded, and the supernatants used for protein quantification by Bradford assay and subsequently for the determination of the activity of the Citrate Synthase enzyme.

The samples were diluted in Tris-buffer (100 mM; pH 8.2) containing 5,5'-dithiobis-2-nitrobenzoic acid (100 µM) and acetyl-coenzyme A (100 µM). The assay was performed in 96 multiwell plates (1 µg of proteins per well) and the reaction started by the addition of oxaloacetic acid solution (500 µM). The reaction was followed spectrophotometrically at 37 °C every 30 s for 15 min at the wavelength of 412 nm (EnSpire, PerkinElmer, Waltham, MA, USA). Citrate synthase activity was determined by comparing the samples activity with a known concentration of the isolated enzyme (Sigma–Aldrich,

St. Louis, MO, USA). Citrate synthase activity was expressed in mU mL<sup>-1</sup>.<sup>[21,22]</sup>

## 2.11. Recording of Colonic Contractile Activity

The contractile activity of colonic muscle preparations was carried out as described in detail by Antonioli et al.,<sup>[20]</sup> with minor changes. Following sacrifice, the colon was immediately removed by an incision above the anal end and placed into Krebs solution. Segments of colon were opened along the mesenteric insertion and mucosal/submucosal layer were removed. Colonic samples were slitted along the longitudinal axis into strips of approximately 4-mm in width and 10-mm in length.

The preparations were set up in organ baths containing Krebs solution at 37 °C, bubbled with 5% CO<sub>2</sub> + 95% O<sub>2</sub>, and connected to isometric transducers (constant load = 0.5 g). The mechanical activity was registered by BIOPAC MP150 (Biomedica Mangoni, Pisa, Italy). The Krebs solution was composed as follow (mM): KCl 4.7, NaCl 113, KH<sub>2</sub>PO<sub>4</sub> 1.2, CaCl<sub>2</sub> 2.5, MgSO<sub>4</sub> 1.2, NaHCO<sub>3</sub> 25, and glucose 11.5 (pH 7.4 ± 0.1). Each preparation was allowed to equilibrate for at least 30 min, with intervening washings at 10 min intervals. A pair of coaxial platinum electrodes was put at 10 mm from the longitudinal axis of each preparation to bring electrical stimulation (ES) by a BM-ST6 stimulator (Biomedica Mangoni, Pisa, Italy). At the end of equilibration period, each preparation was repeatedly challenged with electrical stimuli, and experiments started when reproducible responses were obtained (usually after two or three stimulations).

Thank to previous experiments, the appropriate ES frequency, exogenous substance P (SP), and carbachol (CCh) concentrations were selected.

In the first set of experiments, the total ES at 10 Hz (10-s ES, 0.5 ms, 30 mA) was recorded in colonic samples maintained in standard Krebs solution.

In the second and third set of experiments, cholinergic contractions were recorded. Colonic samples were maintained in Krebs solution containing *N*-ω-nitro-L-arginine methylester (L-NAME, nitric oxide synthase inhibitor, 100 µM), *N*-acetyl-L-tryptophan 3,5-bis(trifluoromethyl) benzylester (L-732138, neurokinin NK1 receptor antagonist, 10 µM), 5-fluoro-3-[2-[4-methoxy-4-[(R)-phenylsulphonyl]methyl]-1-piperidinyl]ethyl]-1H-indole (GR159897, NK2 receptor antagonist, 1 µM), (R)-[[[2-phenyl-4-quinolinyl]carbonyl]amino]-methyl ester benzeneacetic acid (SB218795, NK3 receptor antagonist, 1 µM) and guanethidine (adrenergic blocker 10 µM), in order to assess the neurogenic contraction, and in Krebs solution containing tetrodotoxin (TTX, 1 µM) and challenged with CCh (10 µM), to study the myogenic responses.

The fourth and the fifth series of experiments were set up in order to assess the tachykininergic NK1 stimuli. The neurogenic NK1 contractions were recorded in colonic specimens maintained in Krebs solution containing L-NAME (100 µM), guanethidine (10 µM), GR159897 (1 µM), SB218795 (1 µM), and atropine sulphate (muscarinic receptor antagonist, 1 µM) whereas the myogenic activity was detected maintaining the specimens in TTX-added Krebs solution and stimulating with exogenous SP (1 µM).

## 2.12. Statistical Analysis

GraphPad Prism (GraphPad Prism, version 7.0 from GraphPad Software Inc, San Diego, CA, USA) was used to analyze the data, expressed as mean + SEM. Two-way ANOVA or one-way ANOVA was used to assess statistical significance, followed by Tukey's or Dunnett's post hoc tests. Significant differences were obtained with *p* values <0.05.

## 3. RESULTS

### 3.1. SF68 Counteracts the Body Weight Gain in HFD Mice

At the end of week 4 and week 8, a significant increase of body weight was observed in HFD mice as compared with SD animals (Figure 1a,b). Dietary supplementation with SF68 counteracted significantly the body weight gain in HFD-fed mice (Figure 1a,b). SF68 administration did not affect significantly body weight in SD-fed mice (Figure 1a,b).

### 3.2. Dietary Supplementation with SF68 Reduces Plasmatic IL-1 $\beta$ and LBP Levels

After 8 weeks, mice fed with HFD showed a significant increase in LBP and IL-1 $\beta$  plasma levels as compared with SD animals (Figure 1c,d). The plasma IL-1 $\beta$  levels were significantly reduced in HFD-fed mice administered with SF68 for 4 or 8 weeks (Figure 1d). By contrast, a reduction of LBP plasma levels was observed in obese mice treated for 8 weeks, but not after 4 weeks (Figure 1c).

### 3.3. SF68 Modulates the Intestinal Microbial Communities

SF68 was able to determine significant alterations in the gut microbiota after 8 weeks of administration at both bacterial *phyla* (see Figure 2a) and *genera* levels (see Supplemental Figure S2).

### 3.4. SF68 Reduced Fecal Butyrate Levels and HDAC1 Expression in Obese Mice

Fecal butyrate levels and HDAC1 expression levels were significantly increased in HFD-fed mice (Figure 2b,c). Supplementation with SF68 for 4 or 8 weeks significantly reduced the fecal butyrate concentration and HDAC1 expression levels (Figure 2b,c).

### 3.5. SF68 Ameliorated the Intestinal Inflammation and Expression of Mucins in HFD-Fed Animals

Colonic samples from HFD animals showed a significant increase in MPO and MDA levels (Figure 3a,b), as well as in eosinophil infiltration (Figure 3c) in comparison with SD animals. Furthermore, HFD mice displayed changes in acidic/neutral mucin balance, with a significant decrease in acidic mucins as compared with SD mice (Figure 3d). Such alterations were significantly counteracted by dietary supplementation with SF68 (Figure 3b–d).

### 3.6. SF68 Treatment Ameliorates the Intestinal Barrier Integrity

Mice fed with HFD for 8 weeks showed a significant reduction in colonic ZO-1, occludin, or claudin-1 compared to SD mice (Figure 4a–e). The supplementation with SF68 for 8 weeks determined a significant increase in tight junction protein expression. By contrast, supplementation with SF68 for 4 weeks did not affect tight junction expression (Figure 4a–e).

### 3.7. Supplementation with SF68 Reduced Colonic TLR4 and NF- $\kappa$ B Expression

Colonic tissues from HFD mice displayed a significant increase in TLR4, but not in TLR2 expression (Figure 5a–c). Supplementation with SF68 for 8 weeks significantly reduced TLR4 expression in obese mice (Figure 5a,b). No effect was observed for SF68 on TLR2 expression (Figure 5a,c).

After 8 weeks, colonic tissues from mice fed with HFD diet showed a significant increase in NF- $\kappa$ B levels (Figure 5a,d). Obese animals supplemented with SF68 for 4 or 8 weeks displayed a significant reduction of NF- $\kappa$ B (Figure 5a,d). On the other hand, no significant differences were observed in colonic levels of MyD88 in all experimental groups (Figure 5a,e).

### 3.8. SF68 Supplementation Ameliorates the Expression of Intestinal Butyrate Transporter SMCT1 in Obese Mice

Mice fed with HFD exhibited a significant reduction in the colonic expression of the apical transporter SMCT1, compared to SD mice (Figure 6a). By contrast, the colonic expression of MCT1 (apical) and MCT4 (basolateral) transporters were not affected (Figure 6b,c). Dietary supplementation with SF68 for 4 or 8 weeks normalized the colonic expression of the SMCT1 transporter (Figure 6a), whereas no effect was observed on MCT1 or MCT4 expression (Figure 6b,c).

### 3.9. Citrate Synthase Activity in Intestinal Epithelium

The administration of SF68 to mice fed with SD did not alter the mitochondrial functionality, measured as citrate synthase activity, in intestinal tissues (Figure 6d). By contrast, the citrate synthase activity was significantly reduced in tissues from HFD-fed animals (Figure 6d). Dietary supplementation with SF68 increased significantly the intestinal mitochondrial functionality in obese animals (Figure 6d).

### 3.10. SF68 Supplementation Counteracted Colonic Dysmotility in Obese Mice

During the period of stabilization, the preparations showed rapid spontaneous motor activity that remained stable throughout the experiment and, in most cases, was minimal and did not interfere with the motor responses evoked by the ES (data not shown).

In colon preparations from SD or HFD animals, maintained in standard Krebs solution, the application of electrical stimuli induced contractile responses of comparable magnitude after

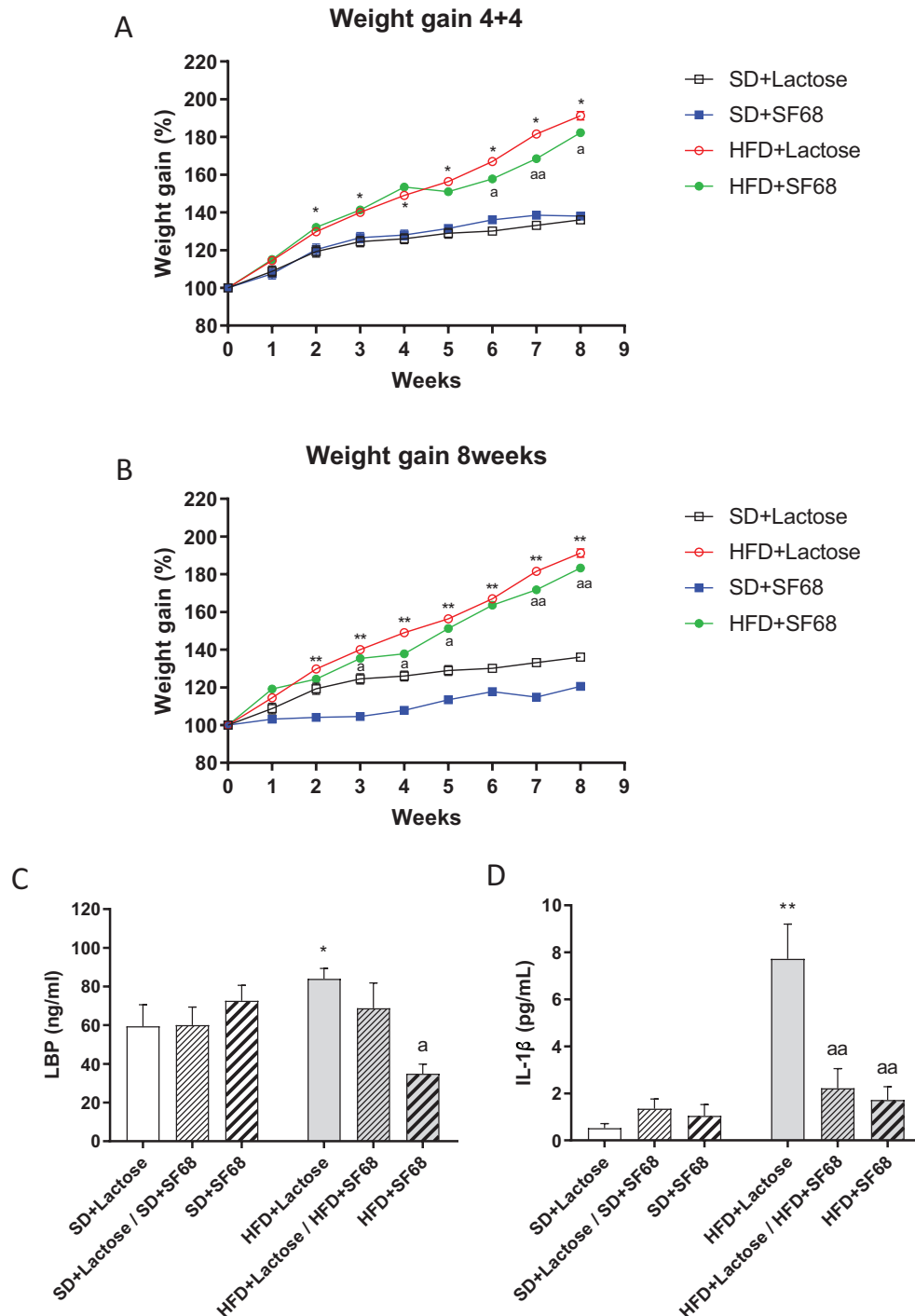


**Figure 1.** a, b) Body weight variations (%), circulating LBP c) and IL-1 $\beta$  d) in mice treated with SD + Lactose, SD + SF68, HFD + Lactose, and HFD + SF68 in the 4 + 4- and 8-weeks therapeutical scheme. All values are presented as mean  $\pm$  SEM ( $n = 10$ ). \* $p < 0.05$  significant difference versus SD + Lactose; \*\* $p < 0.01$  significant difference versus SD + Lactose, <sup>a</sup> $p < 0.05$  significant difference versus HFD + Lactose; <sup>aa</sup> $p < 0.01$  significant difference versus HFD + Lactose. HFD, high-fat diet; IL, interleukin; SD, standard diet; SEM, standard error of the mean.

8 weeks of treatment with SD or HFD (Supplemental Figure S3). In particular, the pharmacological isolation of acetylcholine and SP, the main excitatory systems of enteric nervous system, allowed to observe that colonic tissues from obese mice showed a reduction in cholinergic activity and a concomitant increase in

tachykinergic activity (Supplemental Figure S3). Dietary supplementation with SF68 determined a normalization of colonic contractile responses, restoring the normal cholinergic contractile profile and counteracting the overactivity of the tachykinergic system (Supplemental Figure S3).

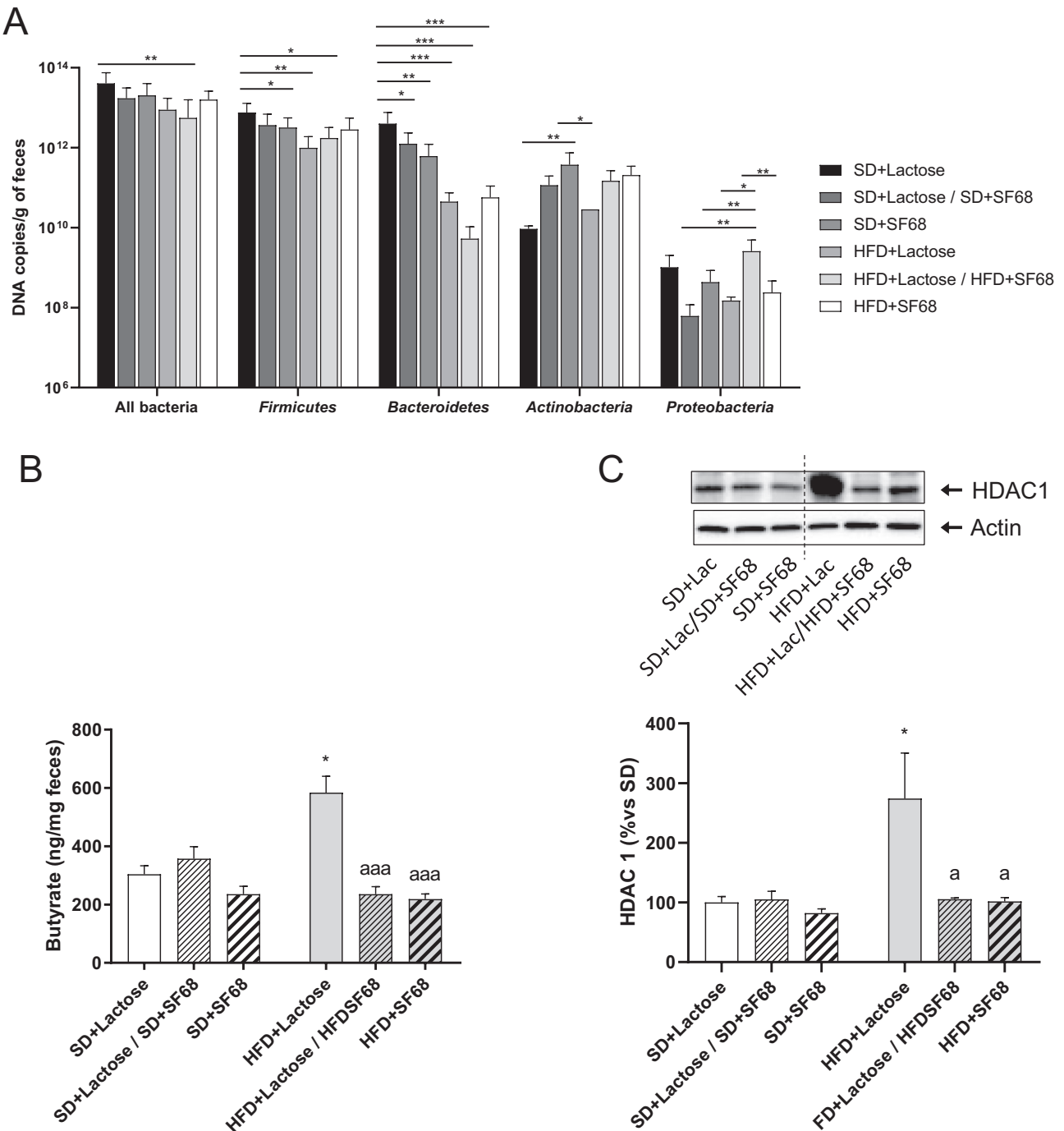


**Figure 2.** a) Bacterial *phyla*, b) butyrate content in feces, and c) representative blot and densitometric analysis of HDAC1 expression in colonic tissues from mice treated with SD + Lactose, SD + SF68, HFD + Lactose, and HFD + SF68 in the 4 + 4- and 8-weeks therapeutical scheme. All values are presented as mean  $\pm$  SEM ( $n = 10$ ). \* $p < 0.05$  significant difference versus SD + Lactose; \*\* $p < 0.01$  significant difference versus SD + Lactose; \*\*\* $p < 0.001$  significant difference versus SD + Lactose; <sup>a</sup> $p < 0.05$  significant difference versus HFD + Lactose, <sup>aaa</sup> $p < 0.001$  significant difference versus HFD + Lactose. HFD, high-fat diet; SD, standard diet; SEM, standard error of the mean.

#### 4. Discussion and Conclusions

Several clinical and preclinical evidence pointed out the alterations of the intestinal epithelial barrier as a critical pathological mechanism in the onset and development of metabolic disorders,

including obesity and type 2 diabetes.<sup>[23]</sup> Indeed, an imbalance in the intestinal barrier structure can flare up into an uncontrollable immune reaction in the enteric microenvironment, fueled by the translocation of immunogenic products.<sup>[23]</sup> The presence of this low-grade enteric and systemic inflammation (also named

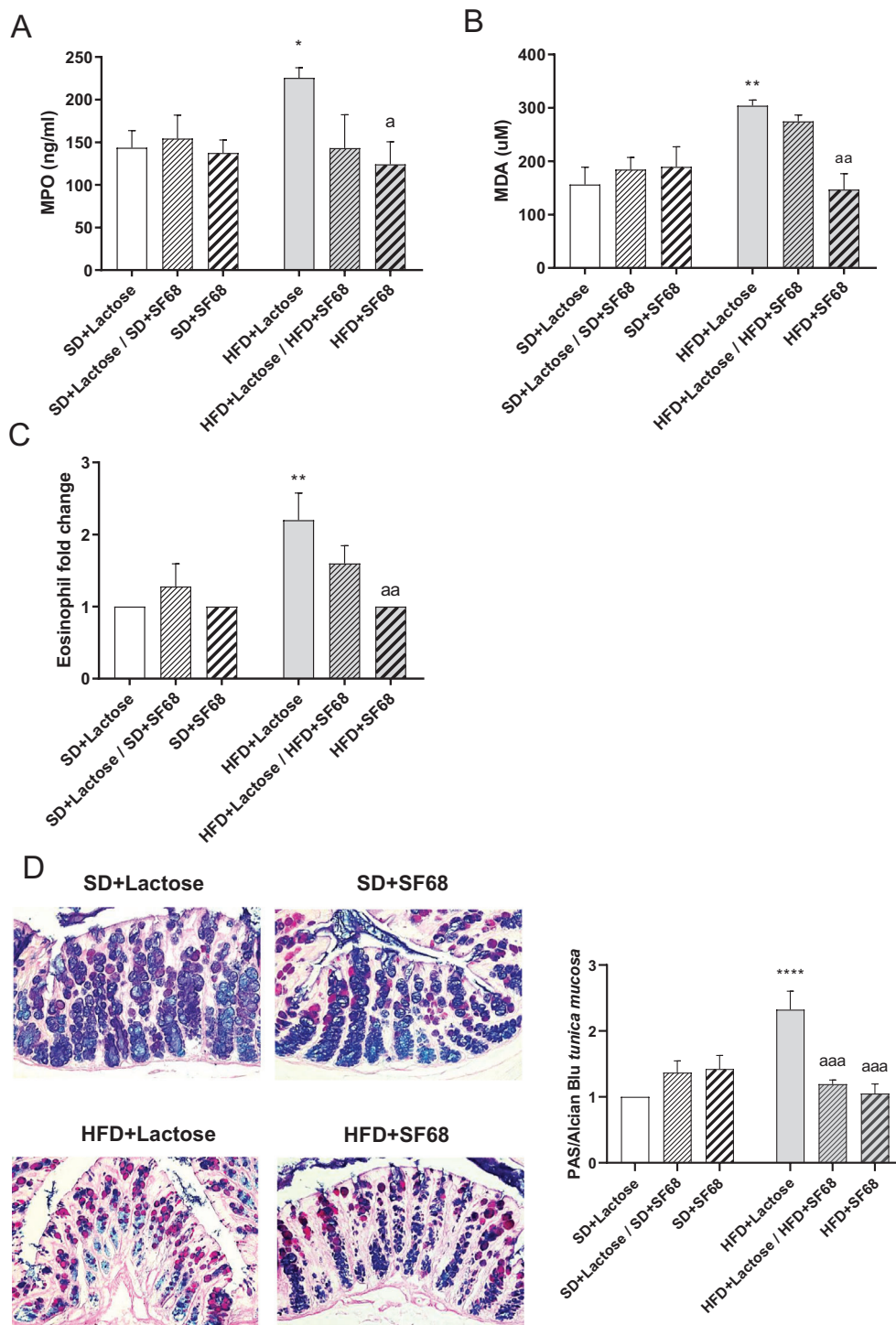


**Figure 3.** a) MPO and b) MDA levels, c) eosinophil density and d) representative images and ratio of neutral (PAS-stained) and acidic (Alcian Blu-stained) mucins expression in colonic tissues from mice treated with SD + Lactose, SD + SF68, HFD + Lactose, and HFD + SF68 in the 4 + 4- and 8-weeks therapeutic scheme. All values are presented as mean  $\pm$  SEM ( $n = 10$ ). \* $p < 0.05$  significant difference versus SD + Lactose; \*\* $p < 0.01$  significant difference versus SD + Lactose; \*\*\*\* $p < 0.0001$  significant difference versus SD + Lactose; <sup>a</sup> $p < 0.05$  significant difference versus HFD + Lactose; <sup>aa</sup> $p < 0.01$  significant difference versus HFD + Lactose; <sup>aaa</sup> $p < 0.001$  significant difference versus HFD + Lactose. HFD, high-fat diet; MDA, malondialdehyde; MPO, myeloperoxidase; PAS, periodic acid-Schiff; SD, standard diet.



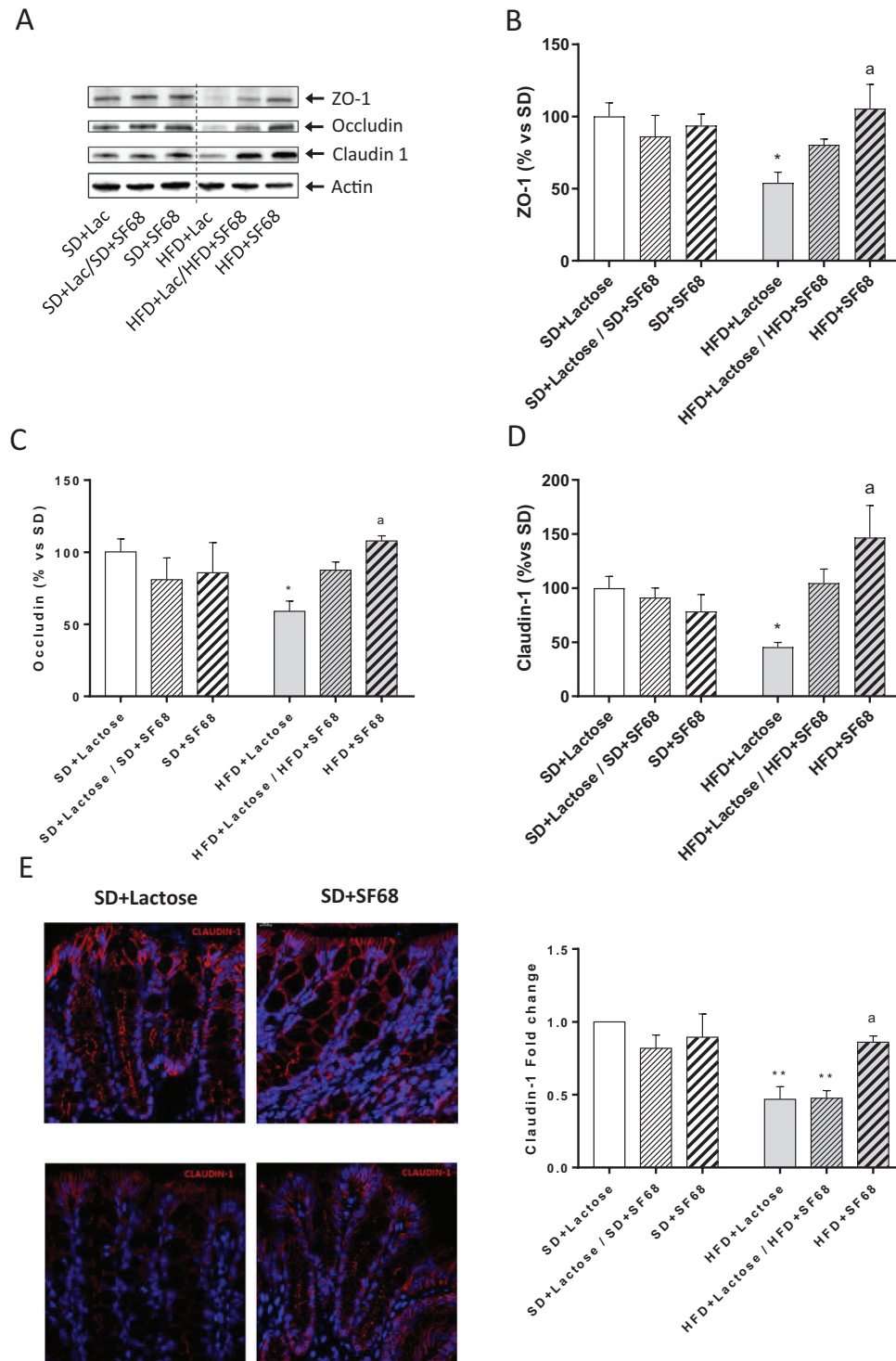


**Figure 4.** Representative blots a) and densitometric analysis of b) ZO-1, c) occludin, and d) claudin-1 and e) claudin-1 expression in colonic tissues from mice treated with SD + Lactose, SD + SF68, HFD + Lactose, and HFD + SF68 in the 4 + 4- and 8-weeks therapeutical scheme. All values are presented as mean  $\pm$  SEM ( $n = 10$ ). \* $p < 0.05$  significant difference versus SD + Lactose; \*\* $p < 0.01$  significant difference versus SD + Lactose; <sup>a</sup> $p < 0.05$  significant difference versus HFD + Lactose. HFD, high-fat diet; SD, standard diet; SEM, standard error of the mean.

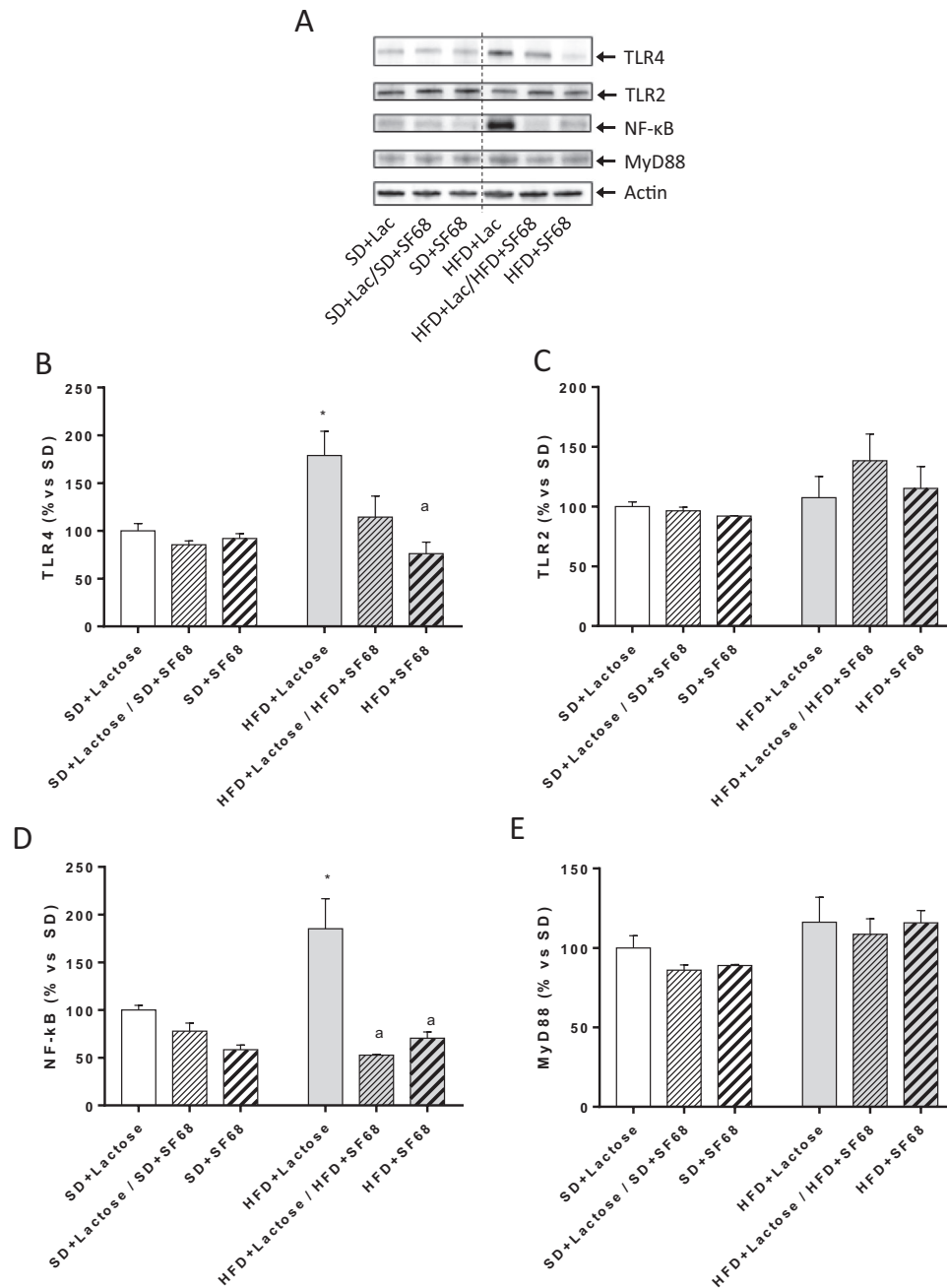


**Figure 5.** Representative blots a) and densitometric analysis of b) TLR4, c) TLR2, d) NF- $\kappa$ B, and e) MyD88 in colonic tissues from mice treated with SD + Lactose, SD + SF68, HFD + Lactose, and HFD + SF68 in the 4 + 4- and 8-weeks therapeutical scheme. All values are presented as mean  $\pm$  SEM ( $n = 10$ ). \* $p < 0.05$  significant difference versus SD + Lactose; <sup>a</sup> $p < 0.05$  significant difference versus HFD + Lactose. HFD, high-fat diet; SD, standard diet; TLR, toll-like receptor.

meta-inflammation) represents the pathophysiological link between obesity and related comorbidities.<sup>[24]</sup> In the last years, the modulation of gut barrier function through nutritional and other interventions, including manipulation of gut microbiota via prebiotics and/probiotics, has emerged as a potential prevention and treatment strategy for the management of metabolic diseases.

Based on these premises, we designed the present study to evaluate the efficacy of SF68 administration in counteracting and

preventing the impairment of gut barrier and the onset of enteric inflammation in a mouse model of diet-induced obesity, characterizing the molecular mechanisms underlying such beneficial effects. Our experiments pointed out three major novel findings: 1) dietary supplementation with SF68 reinforced intestinal epithelial barrier in obese mice; 2) such positive trophic effect is ascribable to the ability of SF68 to improve the transport and utilization of butyrate by the enteric mucosa; and 3) the reinforcement

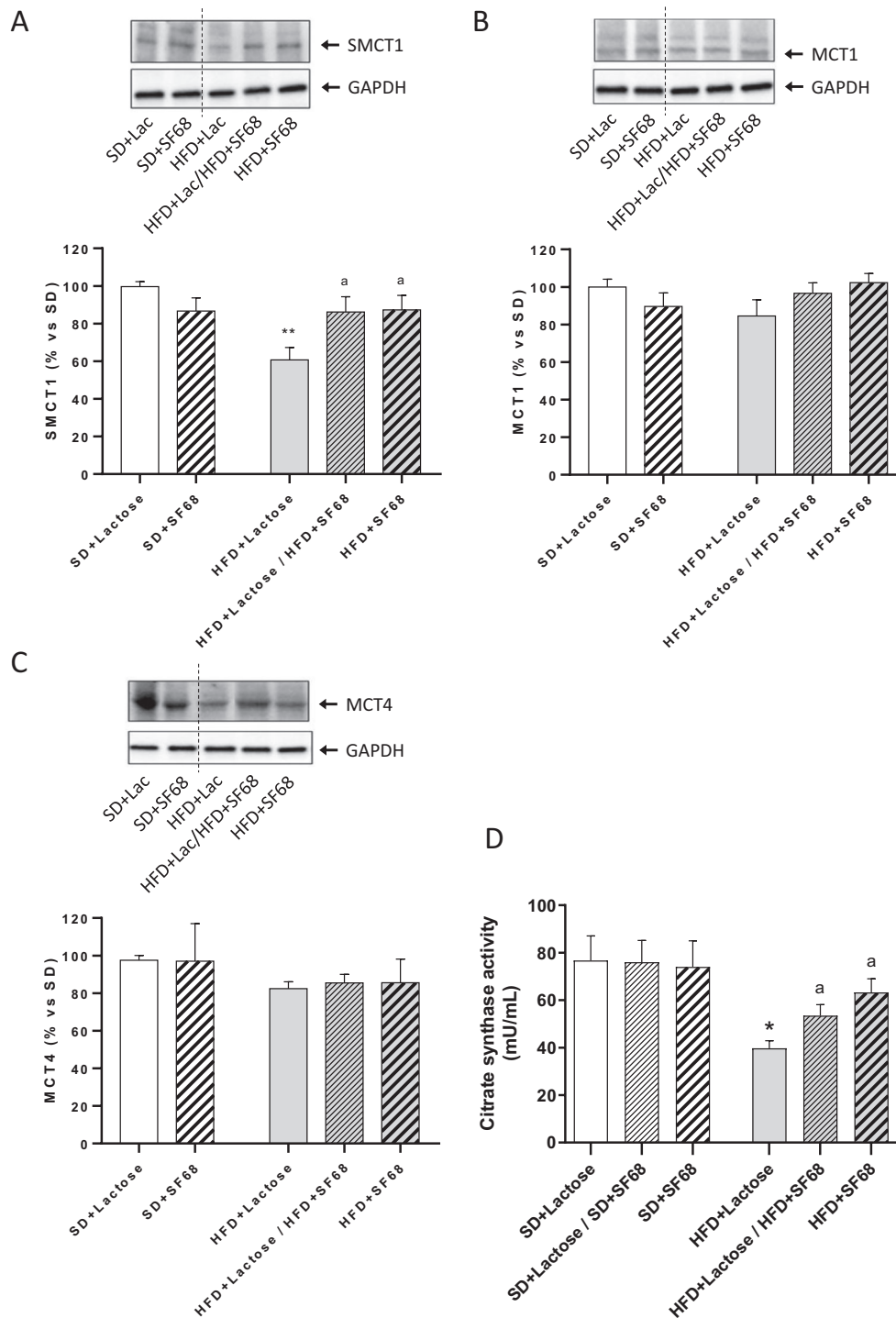


**Figure 6.** Representative blots and densitometric analysis of a) SMCT1, b) MCT1, and c) MCT4 expression and d) citrate synthase activity in mice treated with SD + Lactose, SD + SF68, HFD + Lactose, and HFD + SF68 in the 4 + 4- and 8-weeks therapeutic scheme. All values are presented as mean  $\pm$  SEM ( $n = 10$ ). \* $p < 0.05$  significant difference versus SD + Lactose; \*\* $p < 0.01$  significant difference versus SD + Lactose; <sup>a</sup> $p < 0.05$  significant difference versus HFD + Lactose. HFD, high-fat diet; MCT, monocarboxylate transporter; SD, standard diet; SMCT1, sodium-coupled monocarboxylate transporter 1.

of gut epithelial barrier counteracted body weight increase along with a reduction of enteric inflammation and oxidative stress, followed by an amelioration of the colonic contractile dysfunctions.

To pursue these aims, we employed a murine model of HFD-induced obesity, which displays a considerable face validity with human obesity.<sup>[25]</sup> In this experimental model, accordingly with previous evidence,<sup>[26–28]</sup> we observed that mice fed with a hypercaloric diet developed a significant increase in body weight, the occurrence of a systemic inflammatory condition characterized by high plasma levels of IL-1 $\beta$ , as well as a marked appearance of immune/inflammatory cells and oxidative stress in intestinal tissues, thus corroborating the suitability of this model. Indeed, it is widely recognized that HFD consumption, inducing intestinal dysbiosis, elicited a series of early pathophysiological changes, such as low-grade of intestinal inflammation, a reduction of the antimicrobial peptides expression, an impaired mucus production, secretion and layer's thickness, followed by a decreased expression of tight junction proteins.<sup>[29,30]</sup> In particular, an HFD negatively enriches the gut microflora with barrier-disrupting species, such as *Bacteroides* spp., *Prevotella* spp., *Clostridium* spp., *Oscillobacter* spp., and *Desulfovibrio* spp.<sup>[31]</sup> Variations in the composition of gut microbial communities in mice fed with HFD were also shown in our study, with lower abundances of Firmicutes and Bacteroidetes in comparison with mice fed with SD.

Over the years, it has been observed that the HFD consumption elicited the activation of major inflammatory signals (e.g., TLR-4 dependent), thereby stimulating the secretion of proinflammatory cytokines in the intestinal tissue.<sup>[29]</sup> This is in line to what observed in our experimental model, where obese mice displayed an increased expression of TLR-4, but not TLR-2, in the colon of HFD-fed animals. This increment was associated with the raise of the NF- $\kappa$ B signaling, which plays a critical role for an effective immune response.<sup>[32]</sup> Of note, TLR-4 specifically recognizes bacterial lipopolysaccharide (LPS), and its activation directly alters the intestinal barrier unsettling the tight junction organization via TLR4-CD14-mediated activation of NF- $\kappa$ B.<sup>[13]</sup> In parallel, the activation of the TLR-4/NF $\kappa$ B spurs the expression of several of proinflammatory cytokines that play pivotal roles in altering epithelial barrier.<sup>[31]</sup> Accordingly, we observed a marked immune cell infiltration and oxidative stress in colonic tissues from HFD mice. In this context, the dietary supplementation with SF68 for 8 weeks determined a reduction of TLR-4 and NF $\kappa$ B expression, followed by a marked reduction of immune cell infiltration and oxidative stress in colonic tissue from obese mice, confirmed by the significant decrease in colonic MPO and MDA levels, respectively, thus demonstrating an antiinflammatory and antioxidant activity. In line with this evidence, a previous study described the efficacy of *E. faecium* CFR3003 in exerting a free-radical scavenging effect coupled with reductions in the levels of inflammatory cytokines.<sup>[33]</sup> It is worth to note that a recent paper by Ghazisaeedi et al. described a modulatory effect of SF68 on innate immune signaling pathways. In this paper, the authors conclude that the prior observations of immuno-modulatory effects of SF68 are most likely due to the presence of an active fraction containing arginine deiminase, resulting in arginine deprivation of host cells with subsequent loss of NF- $\kappa$ B and JNK(AP-1) signaling pathway functions.<sup>[34]</sup>

The presence of an inflammatory state in the gut of HFD mice might subsequently exacerbate disruption of the mucus layer barrier and increase epithelial permeability of the gut.

In our results, we found that HFD mice displayed a significant decrease in acidic mucins (Alcian blu positive) and no changes in neutral ones (PAS positive), suggesting an imbalance of neutral/acidic mucin ratio, associated with a reduction of occludin, zonulin-1, and claudin-1 expression, the main tight junctions involved in preserving epithelial barrier integrity. The imbalance of neutral/acidic mucin ratio and epithelial alteration, creating an environment that facilitates the passage of bacterial components (e.g., LPS, peptidoglycan and flagellin) and metabolites from the intestinal lumen to the circulation and peripheral tissues, induces a low-grade systemic inflammation and promotes the onset of a metabolic endotoxemia. In line with this view, we observed an increase of plasma IL-1 $\beta$  and LBP thus confirming the presence of a systemic inflammation as well as an increased intestinal permeability in obese mice. Of note, an elevated serum LPS level is commonly observed in several disorders displaying an increased intestinal permeability as common pathological feature, such as patients with inflammatory bowel diseases (IBDs), irritable bowel syndrome (IBS), celiac disease, or necrotizing enterocolitis.<sup>[35–38]</sup> For this reason, serum LPS is now an accepted surrogate marker for assessing in vivo intestinal permeability. Interestingly the administration of SF68 showed to reinforce significantly the intestinal epithelial barrier, normalizing the expression of tight junction claudin-1 as well as the acidic mucin content altered in obese mice. Of note the altered quantity and chemical composition of mucins may impair the efficacy of the mucus layer in preserving the lining epithelium from a direct contact with intestinal pathogens in HFD mice.

It is well recognized that the bacterial community participates in maintaining intestinal homeostasis through the “training” of the immune system, inhibiting growth of pathogens and pathobionts as well as in maintaining epithelial integrity.<sup>[39]</sup> In this regard, the bacterial species that feed on non-digestible dietary fibers and produce the SCFAs as metabolites seem to play a particularly important role.<sup>[39]</sup> These carboxylic acids with aliphatic tails, including acetate, propionate, and butyrate, are an important fuel for intestinal epithelial cells and are known to strengthen the gut barrier function.<sup>[39]</sup> Interestingly, when considering the fecal butyrate level in our murine model of obesity we observed an increased concentration of butyrate in the feces obtained from HFD-fed mice. This is an intriguing point, since it has been widely demonstrated that butyrate represents the primary energy source employed by colonocytes to maintains intestinal homeostasis through antiinflammatory actions and facilitating the assembly of the tight junction proteins.<sup>[39,40]</sup>

Recent work has demonstrated that butyrate can modulate intestinal macrophage function, that induce differentiation of FoxP3<sup>+</sup> T<sub>reg</sub> cells via a mechanism dependent on retinoic acid, IL-10, and transforming growth factor- $\beta$ ,<sup>[41]</sup> via the inhibition of histone deacetylases.<sup>[42]</sup> Also, set of in vitro studies described that naive T cells under the T<sub>reg</sub>-cell-polarizing conditions incubated with butyrate enhanced histone H3 acetylation in the promoter and conserved non-coding sequence regions of the *Foxp3* locus.<sup>[43]</sup> This evidence suggests that butyrate plays a role in shaping the differentiation of T<sub>reg</sub> cells, referring to a possible mechanism by which host-microbe interactions establish

immunological homeostasis in the digestive tract.<sup>[42,43]</sup> In line with this evidence, we observed that HDAC1 expression, enhanced in HFD-fed animals, was significantly reduced with the SF68 administration, indicating an increase in the butyrate bioavailability in the colon and a possible role in maintaining gut homeostasis.

Physiologically, the absorption of SCFAs, including butyrate, is facilitated by luminal transporters like MCT1 and SMCT1.<sup>[39]</sup> Once internalized into intestinal epithelium butyrate mediated the transcription of genes that are involved in pyruvate dehydrogenase, citric acid cycle, and the respiratory chain.<sup>[44]</sup> In this context, citrate synthase represents a critical player, since it is the first enzyme of the TCA-cycle and catalyzes the condensation of oxaloacetate, a citric acid cycle intermediate, and acetyl-CoA to form citrate, thus preserving the energy status in the intestinal epithelium and, in turn, maintaining the epithelial barrier homeostasis.<sup>[44]</sup> In our study, we hypothesize that the marked luminal presence of butyrate in HFD-fed mice was ascribable to an unsettlement of the butyrate transporters and/or its cellular utilization. This hypothesis has been substantiated by our experiments demonstrating a reduced expression of SMCT1, the main butyrate luminal transporter,<sup>[45]</sup> as well as a significant reduction in citrate synthase activity in the intestinal tissues from HFD-fed mice. Interestingly, obese animals supplemented with SF68 showed an increased expression of SMCT1 and an enhanced activity of citrate synthase, similar to what observed in the intestinal tissues from lean mice. This represents an intriguing point, since it is conceivable that the ameliorative effects of SF68 may be ascribed, at least in part, to the ability of this probiotic to restore a correct absorption and utilization of butyrate by enterocytes. This event would explain the ameliorative effect of SF68 on the expression of tight junctions as well as its anti-inflammatory effect. Indeed, it is well recognized that beyond a trophic activity on epithelial cells, butyrate has a remarkable antiinflammatory effect, promoting the functionalities of M2 macrophages and follicular regulatory T cells<sup>[43]</sup> and inhibiting infiltration by neutrophils.<sup>[46]</sup>

The presence of a bidirectional interactions between immune/inflammatory cells and the enteric nervous system in modulating the enteric motility is well recognized.<sup>[47]</sup> A balanced interplay between the microbiota and the mucosal/neuromuscular intestinal compartment represents the cornerstone of the gut motility homeostasis.<sup>[48]</sup> Several pathological conditions characterized by intestinal dysbiosis, followed by an altered epithelial barrier permeability, are characterized by the development of enteric motor alterations.<sup>[49]</sup> Indeed, the presence of an inflammatory condition in the gut, resulting from a weakening of the epithelial barrier, can alter digestive motility eliciting morphofunctional changes in the enteric neuromuscular compartment.<sup>[50]</sup> In particular, several studies have reported that changes in enteric tachykinergic pathways are actively involved in the pathophysiology of motor digestive disorders associated with inflammatory conditions, e.g., IBDs, diverticulitis, and IBS.<sup>[51,52]</sup> In this regard, a number of epidemiological studies highlighted a high prevalence of enteric motor dysfunction including constipation, abdominal pain syndrome, and IBS in obese subjects.<sup>[53,54]</sup> Similar enteric motor dysfunctions were also reported in preclinical studies performed on HFD obesity model, with a marked reduction of both fecal output and stool water content, thus confirming a link between obesity and constipation.<sup>[28]</sup>

In the present study, we confirmed our previous evidence describing significant alterations of colonic excitatory neuromotility, characterized by a reduced cholinergic response and an exalted tachykinergic pathway.<sup>[27,28,55]</sup> Of note, colonic specimens from obese mice administered with SF68 displayed a pattern of colonic contractions similar to what observed in tissues from animals fed with an SD. This ameliorative effect of SF68 on the colonic motility is likely to be ascribed to the antiinflammatory and antioxidant properties of this probiotic. Indeed, it has been demonstrated that the presence of intestinal inflammation determines a reorganization of neurochemical coding on the enteric neurons, with a reduction of cholinergic nerves<sup>[52]</sup> and an increment of the tachykinergic contractions.<sup>[56]</sup> This prevalence of remodeling of excitatory myenteric neurons, with a shift from mainly cholinergic to more SP positive innervation, may constitute part of the neuronal basis for the altered motility disturbance observed during obesity.<sup>[27,28,55]</sup> In parallel, the restoration of cholinergic contractions with SF68 could also be ascribed to the improved butyrate bioavailability. Indeed, it has been reported that butyrate, increasing the proportion of cholinergic enteric neurons, ameliorates colonic motility and contractile response induced by cholinergic pathways.<sup>[57]</sup> Based on these evidence, SF68 administration, by counteracting the morphofunctional remodeling of enteric neurons, could represent a viable way to manage the intestinal dysmotility typically observed in obese patients.

In conclusion, a dietary supplementation with SF68, especially in the scheme of 8-week treatment, reinforced intestinal epithelial barrier in obese mice, improving butyrate bioavailability in the enteric mucosa. Such strengthening of gut epithelial barrier, reduced the enteric inflammation and oxidative stress, followed by an amelioration of the colonic contractile dysfunctions associated with obesity. In line with this view, despite more addressed studies are needed, it is conceivable that a dietary supplementation with SF68 could exert beneficial effects also in other pathological conditions characterized by an altered intestinal permeability resulting from an unsettlement of tissue butyrate bioavailability such as IBDs, IBS, or visceral pain.<sup>[58–60]</sup>

## Supporting Information

Supporting Information is available from the Wiley Online Library or from the author.

## Acknowledgements

To, and in memory of, Corrado Blandizzi, for trusting in critical moments. Open Access Funding provided by Universita degli Studi di Pisa within the CRUI-CARE Agreement.

## Conflict of Interest

This study was supported by a grant from Cerbios-Pharma SA. The use of SF68 in the management of inflammatory alterations of intestinal mucosa in the presence of obesity has been patented (102022000013138).

## Author Contributions

L.B., V.D., and C.P. contributed equally to the manuscript. L.B., V.D.A., C.D.S., C.I., C.S., A.M., L.F., G.C., M.C., and A.P. carried out the experiment. C.P., M.F., V.C., E.G., R.C., A.A., and L.A. designed the study. L.B.,

V.D.A., C.D.S., and N.B. processed the experimental data, performed the analysis, drafted the manuscript, and designed the figures. All authors discussed the results and contributed to the final manuscript

## Data Availability Statement

Data will be made available upon request.

## Keywords

butyrate, intestinal epithelial barrier, obesity, SF68, tight junctions

Received: November 29, 2022

Revised: February 7, 2023

Published online:

- [1] L. M. Jaacks, S. Vandevijvere, A. Pan, C. J. McGowan, C. Wallace, F. Imamura, D. Mozaffarian, B. Swinburn, M. Ezzati, *Lancet Diabetes Endocrinol.* **2019**, *7*, 231.
- [2] G. S. Hotamisligil, *Nature* **2006**, *444*, 860. <https://doi.org/10.1038/nature05485>
- [3] J. R. Marchesi, D. H. Adams, F. Fava, G. D. A. Hermes, G. M. Hirschfeld, G. Hold, M. N. Quraishi, J. Kinross, H. Smidt, K. M. Tuohy, L. V. Thomas, E. G. Zoetendal, A. Hart, *Gut* **2016**, *65*, 330.
- [4] D. Zheng, T. Liwinski, E. Elinav, *J. Reticuloendothel Soc.* **2020**, *30*, 492.
- [5] P. D. Cani, J. Amar, M. A. Iglesias, M. Poggi, C. Knauf, D. Bastelica, A. M. Neyrinck, F. Fava, K. M. Tuohy, C. Chabo, A. Waget, E. Delmée, B. Cousin, T. Sulpice, B. Chamontin, J. Ferrières, J. F. Tanti, G. R. Gibson, L. Casteilla, N. M. Delzenne, M. C. Alessi, R. Burcelin, *Diabetes* **2007**, *56*, 1761.
- [6] M. J. A. Saad, A. Santos, P. O. Prada, *Physiology* **2016**, *31*, 283.
- [7] K. N. Kim, Y. Yao, S. Y. Ju, *Nutrients* **2019**, *11*, 2512. <https://doi.org/10.3390/nu11102512>
- [8] T. P. M. Scheithauer, E. Rampanelli, M. Nieuwdorp, B. A. Vallance, C. B. Verchere, D. H. van Raalte, H. Herrema, *Front. Immunol.* **2020**, *11*, 571731. <https://doi.org/10.3389/fimmu.2020.571731>
- [9] D. K. Dahiya, M. P. Renuka, U. K. Shandilya, T. Dhewa, N. Kumar, S. Kumar, A. K. Puniya, P. Shukla, *Front. Microbiol.* **2017**, *8*, 563. <https://doi.org/10.3389/fmicb.2017.00563>
- [10] K. Ukibe, M. Miyoshi, Y. Kadooka, *J. Nutr.* **2015**, *144*, 1180. <https://doi.org/10.1017/S0007114515002627>
- [11] M. Miyoshi, A. Ogawa, S. Higurashi, Y. Kadooka, *Eur. J. Nutr.* **2014**, *53*, 599. <https://doi.org/10.1007/s00394-013-0568-9>
- [12] K. Mazloom, I. Siddiqi, M. Covasa, *Nutrients* **2019**, *11*, 258. <https://doi.org/10.3390/nu11020258>
- [13] A. Lewenstein, G. Frigerio, M. Moroni, *Curr. Ther. Res.* **1979**, *26*, 967.
- [14] P. F. Wunderlich, L. Braun, I. Fumagalli, V. D'apuzzo, F. Heim, M. Karly, R. Lodi, G. Politta, F. Vonbank, L. Zeltner, *J. Int. Med. Res.* **1989**, *17*, 333.
- [15] C. M. A. P. Franz, M. Huch, H. Abriouel, W. Holzapfel, A. Gálvez, *Int. J. Food Microbiol.* **2011**, *151*, 125.
- [16] W. Holzapfel, A. Arini, M. Aeschbacher, R. Coppolecchia, B. Pot, *Benef. Microbes* **2018**, *9*, 375.
- [17] P. Sun, J. Wang, Y. Jiang, *Food Chem.* **2010**, *123*, 63.
- [18] L. Antonioli, V. Caputi, M. Fornai, C. Pellegrini, D. Gentile, M. C. Giron, G. Orso, N. Bernardini, C. Segnani, C. Ippolito, B. Csóka, G. Haskó, Z. H. Németh, C. Scarpignato, C. Blandizzi, R. Colucci, *Int. J. Obes.* **2019**, *43*, 331. <https://doi.org/10.1038/s41366-018-0166-2>
- [19] S. K. Lindén, T. H. J. Florin, M. A. McGuckin, *PLoS ONE* **2008**, *3*, e3952. <https://doi.org/10.1371/JOURNAL.PONE.0003952>
- [20] L. Antonioli, V. D'Antongiovanni, C. Pellegrini, M. Fornai, L. Benvenuti, A. di Carlo, R. van den Wijngaard, V. Caputi, S. Cerantola, M. C. Giron, Z. H. Németh, G. Haskó, C. Blandizzi, R. Colucci, *FASEB J.* **2020**, *34*, 5512.
- [21] C. Pellegrini, S. Daniele, L. Antonioli, L. Benvenuti, V. D'antongiovanni, R. Piccarducci, D. Pietrobono, V. Citi, E. Piragine, L. Flori, C. Ippolito, C. Segnani, P. Palazon-Riquelme, G. Lopez-Castejon, A. Martelli, R. Colucci, N. Bernardini, M. L. Trincavelli, V. Calderone, C. Martini, C. Blandizzi, M. Fornai, *Int. J. Mol. Sci.* **2020**, *21*, 3523.
- [22] V. D'Antongiovanni, C. Pellegrini, L. Antonioli, L. Benvenuti, C. di Salvo, L. Flori, R. Piccarducci, S. Daniele, A. Martelli, V. Calderone, C. Martini, M. Fornai, *Front. Pharmacol.* **2021**, *12*, 748021. <https://doi.org/10.3389/FPHAR.2021.748021>
- [23] L. Massier, M. Blüher, P. Kovacs, R. M. Chakaroun, *Front. Endocrinol. (Lausanne)* **2021**, *12*, 616506. <https://doi.org/10.3389/FENDO.2021.616506>
- [24] B. R. Ely, Z. S. Clayton, C. E. McCurdy, J. Pfeiffer, C. T. Minson, *Temperature (Austin)* **2017**, *5*, 9.
- [25] M. Kleinert, C. Clemmensen, S. M. Hofmann, M. C. Moore, S. Renner, S. C. Woods, P. Huypens, J. Beckers, M. H. de Angelis, A. Schürmann, M. Bakhti, M. Klingenspor, M. Heiman, A. D. Cherrington, M. Ristow, H. Lickert, E. Wolf, P. J. Havel, T. D. Müller, M. H. Tschöp, *Nat. Rev. Endocrinol.* **2018**, *14*, 140.
- [26] K. A. Kim, W. Gu, I. A. Lee, E. H. Joh, D. H. Kim, *PLoS ONE* **2012**, *7*, e47713. <https://doi.org/10.1371/JOURNAL.PONE.0047713>
- [27] L. Antonioli, V. D'Antongiovanni, C. Pellegrini, M. Fornai, L. Benvenuti, A. di Carlo, R. van den Wijngaard, V. Caputi, S. Cerantola, M. C. Giron, Z. H. Németh, G. Haskó, C. Blandizzi, R. Colucci, *FASEB J.* **2020**, *34*, 5512.
- [28] L. Antonioli, V. Caputi, M. Fornai, C. Pellegrini, D. Gentile, M. C. Giron, G. Orso, N. Bernardini, C. Segnani, C. Ippolito, B. Csóka, G. Haskó, Z. H. Németh, C. Scarpignato, C. Blandizzi, R. Colucci, *Int. J. Obes. (Lond.)* **2019**, *43*, 331.
- [29] J. R. Araújo, J. Tomas, C. Brenner, P. J. Sansonetti, *Biochimie* **2017**, *141*, 97.
- [30] R. E. Ley, F. Bäckhed, P. Turnbaugh, C. A. Lozupone, R. D. Knight, J. I. Gordon, *Proc. Natl. Acad. Sci. USA* **2005**, *102*, 11070.
- [31] M. Rohr, C. Narasimhulu, T. Rudeski-Rohr, S. Parthasarathy, *Adv. Nutr.* **2020**, *11*, 77.
- [32] V. McGuire, J. Arthur, *Front. Immunol.* **2015**, *6*, 607. <https://doi.org/10.3389/FIMMU.2015.00607>
- [33] G. Divyashri, G. Krishna, N. Muralidhara, S. Prapulla, *J. Med. Microbiol.* **2015**, *64*, 1527.
- [34] F. Ghazisaeedi, J. Meens, B. Hansche, S. Maurischat, P. Schwerk, R. Goethe, L. H. Wieler, M. Fulde, K. Tedin, *Gut Microbes* **2022**, *14*, 2106105. <https://doi.org/10.1080/19490976.2022.2106105>
- [35] S. Ghosh, J. Wang, P. Yannie, S. Ghosh, *J. Endocr. Soc.* **2020**, *4*, bvz039. <https://doi.org/10.1210/JENDSO/BVZ039>
- [36] H. Fukui, *Inflamm. Intest. Dis.* **2016**, *1*, 135.
- [37] D. Chatterton, D. Nguyen, S. Bering, P. Sangild, *Int. J. Biochem. Cell Biol.* **2013**, *45*, 1730.
- [38] D. Cardoso-Silva, D. Delbue, A. Itzlinger, R. Moerkens, S. Withoff, F. Branchi, M. Schumann, *Nutrients* **2019**, *11*, 2325. <https://doi.org/10.3390/NU1102325>
- [39] D. Parada Venegas, M. de la Fuente, G. Landskron, M. González, R. Quera, G. Dijkstra, H. Harmsen, K. Faber, M. Hermoso, *Front. Immunol.* **2019**, *10*, 277. <https://doi.org/10.3389/FIMMU.2019.00277>
- [40] L. Peng, Z. Li, R. Green, I. Holzman, J. Lin, *J. Nutr.* **2009**, *139*, 1619.
- [41] T. L. Denning, Y. C. Wang, S. R. Patel, I. R. Williams, B. Pulendran, *Nat. Immunol.* **2007**, *8*, 1086.
- [42] P. V. Chang, L. Hao, S. Offermanns, R. Medzhitov, *Proc. Natl. Acad. Sci. USA* **2014**, *111*, 2247.

- [43] Y. Furusawa, Y. Obata, S. Fukuda, T. A. Endo, G. Nakato, D. Takahashi, Y. Nakanishi, C. Uetake, K. Kato, T. Kato, M. Takahashi, N. N. Fukuda, S. Murakami, E. Miyauchi, S. Hino, K. Atarashi, S. Onawa, Y. Fujimura, T. Lockett, J. M. Clarke, D. L. Topping, M. Tomita, S. Hori, O. Ohara, T. Morita, H. Koseki, J. Kikuchi, K. Honda, K. Hase, H. Ohno, *Nature* **2013**, *5000*, 446. <https://doi.org/10.1038/nature12721>
- [44] S. Vanhoutvin, F. Troost, H. Hamer, P. Lindsey, G. Koek, D. Jonkers, A. Kodde, K. Venema, R. Brummer, *PLoS ONE* **2009**, *4*, e6759. <https://doi.org/10.1371/JOURNAL.PONE.0006759>
- [45] N. Gupta, P. Martin, P. Prasad, V. Ganapathy, *Life Sci.* **2006**, *78*, 2419.
- [46] C. Chen, L. Vitetta, *Immune Netw.* **2020**, *20*, e15. <https://doi.org/10.4110/IN.2020.20.E15>
- [47] K. Margolis, M. Gershon, *Trends Neurosci.* **2016**, *39*, 614.
- [48] J. Dalziel, N. Spencer, W. Young, *Int. J. Biochem. Cell Biol.* **2021**, *134*, 105963. <https://doi.org/10.1016/J.BIOCEL.2021.105963>
- [49] J. König, J. Wells, P. Cani, C. García-Ródenas, T. MacDonald, A. Mercenier, J. Whyte, F. Troost, R. Brummer, *Clin. Transl. Gastroenterol.* **2016**, *7*, e196. <https://doi.org/10.1038/CTG.2016.54>
- [50] W. Khan, S. Collins, *Clin. Exp. Immunol.* **2006**, *143*, 389.
- [51] W. ter Beek, I. Biemond, E. Muller, M. van den Berg, C. Lamers, *Neuropeptides* **2007**, *41*, 301.
- [52] M. Neunlist, P. Aubert, C. Toquet, T. Oreshkova, J. Barouk, P. Lehur, M. Schemann, J. Galmiche, *Gut* **2003**, *52*, 84.
- [53] M. Fysekidis, M. Bouchoucha, H. Bihan, G. Reach, R. Benamouzig, J. M. Catheline, *Obes. Surg.* **2012**, *22*, 403. <https://doi.org/10.1007/s11695-011-0396-z>
- [54] D. le Pluart, J. M. Sabaté, M. Bouchoucha, S. Hercberg, R. Benamouzig, C. Julia, *Aliment. Pharmacol. Ther.* **2015**, *41*, 758. <https://doi.org/10.1111/apt.13143>
- [55] V. D'Antongiovanni, L. Benvenuti, M. Fornai, C. Pellegrini, R. van den Wijngaard, S. Cerantola, M. C. Giron, V. Caputi, R. Colucci, G. Haskó, Z. H. Németh, C. Blandizzi, L. Antonioli, *Cells* **2020**, *9*, 1245. <https://doi.org/10.3390/cells9051245>
- [56] C. Pellegrini, M. Fornai, L. Benvenuti, R. Colucci, V. Caputi, P. Palazon-Riquelme, M. Giron, A. Nericcio, F. Garelli, V. D'Antongiovanni, C. Segnani, C. Ippolito, M. Nannipieri, G. Lopez-Castejon, P. Pelegrin, G. Haskó, N. Bernardini, C. Blandizzi, L. Antonioli, *Br. J. Pharmacol.* **2021**, *178*, 3924. <https://doi.org/10.1111/BPH.15532>
- [57] R. Soret, J. Chevalier, P. de Coppet, G. Poupeau, P. Derkinderen, J. Segain, M. Neunlist, *Gastroenterology* **2010**, *138*, 1772. <https://doi.org/10.1053/J.GASTRO.2010.01.053>
- [58] R. Thibault, F. Blachier, B. Darcy-Vrillon, P. de Coppet, A. Bourreille, J. Segain, *Inflamm. Bowel Dis.* **2010**, *16*, 684.
- [59] E. Ferrer-Picón, I. Dotti, A. Corraliza, A. Mayorgas, M. Esteller, J. Perales, E. Ricart, M. Masamunt, A. Carrasco, E. Tristán, M. Esteve, A. Salas, *Inflamm. Bowel Dis.* **2020**, *26*, 43.
- [60] R. Bonomo, T. Cook, C. Gavini, C. White, J. Jones, E. Bovo, A. Zima, I. IBrown, L. Dugas, E. Zakharian, G. Aubert, F. Alonzo, N. Calcutt, V. Mansuy-Aubert, *Proc. Natl. Acad. Sci. USA* **2020**, *117*, 26482.